Med Bio Eng Comput (2008) 46:101–108
DOI 10.1007/s11517-007-0303-x

ORIGINAL ARTICLE

New method for analysing sensitivity distributions of electroencephalography measurements

Juho Väisänen · Outi Väisänen · Jaakko Malmivuo · Jari Hyttinen

Received: 8 March 2007 / Accepted: 10 December 2007 / Published online: 10 January 2008

Abstract In this paper, we introduce a new modelling related parameter called region of interest sensitivity ratio (ROISR), which describes how well the sensitivity of an electroencephalography (EEG) measurement is concentrated within the region of interest (ROI), i.e. how specific the measurement is to the sources in ROI. We demonstrate the use of the concept by analysing the sensitivity distributions of bipolar EEG measurement. We studied the effects of interelectrode distance of a bipolar EEG lead on the ROISR with cortical and non-cortical ROIs. The sensitivity distributions of EEG leads were calculated analytically by applying a three-layer spherical head model. We suggest that the developed parameter has correlation to the signal-to-noise ratio (SNR) of a measurement, and thus we studied the correlation between ROISR and SNR with 254-channel visual evoked potential (VEP) measurements of two testees. Theoretical simulations indicate that source orientation and location have major impact on the specificity and therefore they should be taken into account when the optimal bipolar electrode configuration is selected. The results also imply that the new ROISR method bears a strong correlation to the SNR of measurement and can thus be applied in the future studies to efficiently evaluate and optimize EEG measurement setups.

Keywords Electroencephalography · Modelling · Region of interest sensitivity ratio · Sensitivity distribution · Signal-to-noise ratio

J. Väisänen (✉) · O. Väisänen · J. Malmivuo · J. Hyttinen
Ragnar Granit Institute, Tampere University of Technology, P.O. Box 692, 33101 Tampere, Finland
e-mail: juho.vaisanen@tut.fi

1 Introduction

The objective in electroencephalography (EEG) measurements is to register signals arising from sources in a certain region of interest (ROI), e.g. an area where evoked responses are generated in the brain. The sensitivity of an ideal measurement should focus on and be greater on these target areas in comparison to other areas of the volume conductor, thus yielding more specific measurements.

The locations of the measurement electrodes have a prominent effect on the measurement sensitivity. In clinical EEG the traditional electrode setup has been the 10-20-system, while today there are also commercial systems with up to 256 electrodes. These days new technologies enable the use of high numbers of electrodes, but in some cases, such as emergency room EEG and implantable or portable monitoring systems, it is essential to reduce the number of electrodes to minimum. The selection of ideal electrode locations is critical when selecting the measurement system with optimal spatial sensitivity properties. To support this selection, the qualities of various electrode systems should be characterized by different variables related for example, to the sensitivity distributions of electrode set-ups.

Previously, only a few parameters have been applied in the analysis of sensitivity distributions of bioelectric measurements. One of them is the half-sensitivity volume (HSV) [13] that defines the volume in which the measurement sensitivity is concentrated. It has been applied in analysing differences in EEG and MEG measurements [14]. Also, relative differences in sensitivity distributions have been applied in analysis of the sensitivity distributions of implantable ECG monitors [24].

Methods that can be applied to describe how well the measurement sensitivity of a measurement lead is

concentrated on some ROI have not been introduced previously. It would be important to apply the optimal measurement configuration to obtain all information of these sources with high signal-to-noise ratio (SNR). Due to lack of such methods of analysis, it has been complicated to compare the quality of the measurement set-ups with modelling-based approaches when selecting the optimal configurations

The present paper introduces and demonstrates the use of a parameter called region of interest sensitivity ratio (ROISR) in analysing EEG measurements. The ROISR is applied to characterize how well the sensitivities of different bipolar EEG measurement leads are concentrated in the ROI compared to other source regions. In the application of ROISR parameter, it is assumed that the required signal is generated by the sources within ROI and other sources in the volume conductor produce noise to the measurement. We thus assume that the ROISR correlates with the SNR of a measurement. In addition to studying the specificity of different bipolar leads, this paper presents a preliminary EEG study to evaluate the correlation between ROISR and SNR.

2 Materials and methods

2.1 Lead field and reciprocity theorem

The sensitivity distributions of measurement leads in the volume conductor can be illustrated with lead fields as defined by McFee and Johnston [15]. The lead vectors define the relationship between the measured signal in the lead and the current sources in the volume conductor following Eq. 1 [12]. In the optimal measurements the lead vectors and current source vectors are oriented parallel.

$$V_{\mathrm{LE}} = \int \frac{1}{\sigma}\overline{J}_{\mathrm{LE}} \bullet \overline{J}_{\mathrm{i}}\mathrm{d}v = \int \frac{1}{\sigma} \cdot \left|\overline{J}_{\mathrm{LE}}\right| \cdot \left|\overline{J}_{\mathrm{i}}\right| \cdot \cos(\alpha)\mathrm{d}v, \quad (1)$$

where V_{LE} is the lead voltage, $\overline{J}_{\mathrm{LE}}$ is the lead field $\left[\frac{1}{\mathrm{cm}^2}\right]$, $\overline{J}_{\mathrm{i}}$ is the current source density vector $\left[\frac{A}{\mathrm{cm}^2}\right]$, σ is the conductivity at the source location in the volume conductor $\left[\frac{1}{\Omega\mathrm{cm}}\right]$, and α is the angle between lead vector and source vector. $|\,.\,|$ is the L2-norm.

The lead field in the volume conductor can be established by applying the reciprocity theorem of Helmholtz. The current field in the volume conductor raised by the reciprocal unit current ($I_{\mathrm{r}} = 1$ A) applied to the measurement electrodes corresponds to the lead current density and hence to the lead field $\overline{J}_{\mathrm{LE}}$ [15]. The lead field defines the magnitude and direction of sensitivity of the measurement lead at all source locations within the volume conductor.

2.2 The concept of region of interest sensitivity ratio

Equation 2 defines ROISR as a ratio between average sensitivity of a predefined ROI volume and the average sensitivity at the rest of the source volume, hereafter called as a nonROI volume. For example, in the case of EEG the nonROI volume consists of the brain volume excluding the ROI volume. ROISR, thus defines how well the measurement sensitivity is concentrated within the selected ROI, i.e. how specific the measurement is to the signals generated within the ROI.

$$\mathrm{ROISR} = \frac{\frac{1}{V_{\mathrm{ROI}}}\int_{V_{\mathrm{ROI}}} \left|\overline{J}_{\mathrm{LE}}\right|\mathrm{d}v}{\frac{1}{V_{\mathrm{nonROI}}}\int_{V_{\mathrm{nonROI}}} \left|\overline{J}_{\mathrm{LE}}\right|\mathrm{d}v}, \quad (2)$$

where V_{ROI} is the ROI source volume [cm^3] and V_{nonROI} is the nonROI source volume [cm^3].

The ROISR in (Eq. 2) is obtained by taking into account the magnitudes of the lead vectors within the ROI and nonROI volumes. This approach is most suitable in cases where the sensitivity distribution is optimally oriented, i.e. cos (α) in (Eq. 1) equals one or in cases where the directions of the sources are unknown. The angles between the lead vectors and the current source vectors within ROI or nonROI should be taken into account whenever these are known, thus enabling more precise calculations.

For example, it has been recognized that measurable EEG potentials are generated by pyramidal neurons of same orientation and the sources are described with equivalent dipoles [17, 18]. In this case, the direction of equivalent source within the ROI is known but the directions of sources within nonROI are still unknown. Thus the directions of sensitivities within the ROI can be applied in the calculation of ROISR. However, because the orientations of the noise sources in any measurement are almost impossible to know, the worst-case approximation is that they are oriented parallel to the lead vectors. These principles are applied in Eq. 3, describing a case where the angles between current source vectors and lead vectors within ROI are known.

$$\mathrm{ROISR}_{\alpha} = \frac{\frac{1}{V_{\mathrm{ROI}}}\int_{V_{\mathrm{ROI}}} \left|\overline{J}_{\mathrm{LE}}\right| \cdot \cos(\alpha)\mathrm{d}v}{\frac{1}{V_{\mathrm{nonROI}}}\int_{V_{\mathrm{nonROI}}} \left|\overline{J}_{\mathrm{LE}}\right|\mathrm{d}v}, \quad (3)$$

where α is angle between the current source vector and lead vector at each location within ROI.

In (Eqs. 2 and 3), the averages of sensitivities within the ROI and nonROI volumes are applied in the ROISR calculation. This approach is applied because, the source distribution within the volume conductor is not known exactly and thus it cannot be stated if the ROI contains only the sources of interest or if these sources fill the whole ROI. There is the same problem with sources in nonROI; the

estimation of noise source distribution is even more difficult.

2.3 ROISR analysis of bipolar EEG leads

We applied the new ROISR parameter in analyzing the effects of interelectrode distance on the specificities of bipolar EEG leads. We calculated the sensitivity distributions of 70 bipolar EEG leads whose interelectrode distances varied from 180° to 2.57°. The sensitivity distributions were calculated within the brain volume of a three-layer spherical head model with the analytical method introduced by Rush and Driscoll [21]. The model includes the layers of scalp, skull and brain, with radii of 92, 85 and 80 mm, respectively. The resolution of the model is 2 mm × 2 mm × 2 mm containing altogether 267,730 nodes. Each node in the model describes a 8 mm^3 volume in the brain region. There is no certainty of the correct scalp/brain/skull resistivity ratio, and a variety of values have been introduced in different studies [7, 9, 19, 21]. We executed our calculations with 1/15/1 scalp/skull/brain resistivity ratio [19].

In addition, we studied how ROI location affects the specificities of bipolar leads and thus calculated the ROISRs for two different ROIs, one lying on the cortex and the other deeper in the brain. Both ROIs were spherical volumes with a 20 mm radius. The coordinates for the centre of the ROI lying on the cortex were $x = 0$ mm, $y = 0$ mm and $z = 80$ mm and for the deeper ROI $x = 0$ mm, $y = 0$ mm and $z = 30$ mm. Fig. 1 presents two bipolar electrode pairs with the 5.14° and 180° electrode distances applied in this study, and the locations of the ROIs in the brain in a 2D *yz*-plane. We studied the effects of electrode distance with three different assumptions about the source orientation within ROI. ROISRs were calculated with unknown source orientation by applying (Eq. 2) and with known source orientation by applying (Eq. 3). For simplicity, the known source orientations were selected to be positive *y*- and *z*-directions illustrated in Fig. 1.

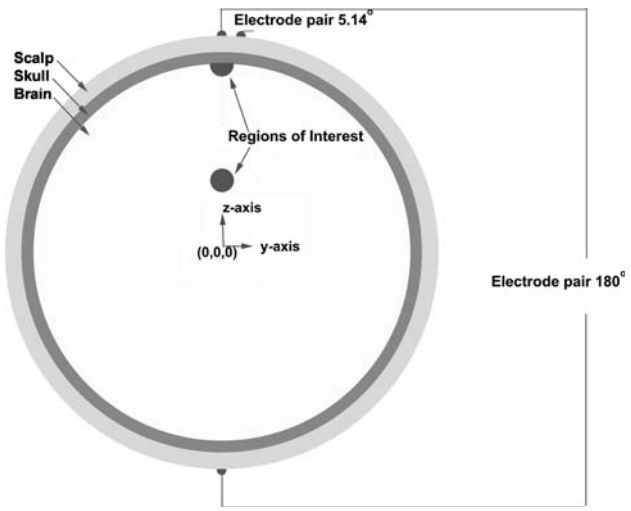

Fig. 1 Cross-section of the three-layer spherical head model with 5.14° and 180° electrode distances. The cortical ROI and non-cortical ROI located within the brain are indicated with *dark grey circles*

2.4 Relationship between ROISR and SNR

We claim that the ROISR parameter has a strong correlation to the SNR of a bioelectric measurement, here EEG. Eq. 4 describes the SNR of a measurement based on lead vector approach (Eq.1). We assume that required signal is raised by sources lying in the ROI and unwanted noise originates from the sources in the nonROI volume.

$$\mathrm{SNR} = \frac{\mathrm{Signal}}{\mathrm{Noise}} = \frac{\int_{V_{\mathrm{ROI}}} \frac{1}{\sigma} \left|\overline{J}_{\mathrm{LE}}\right| \cdot \left|\overline{J}_{\mathrm{i}}\right| \cdot \cos(\alpha) \mathrm{d}v}{\int_{V_{\mathrm{nonROI}}} \frac{1}{\sigma} \left|\overline{J}_{\mathrm{LE}}\right| \cdot \left|\overline{J}_{\mathrm{i}}\right| \cdot \cos(\beta) \mathrm{d}v} \approx \frac{\left|\overline{J}_{\mathrm{i}}\right| \cdot \int_{V_{\mathrm{ROI}}} \left|\overline{J}_{\mathrm{LE}}\right| \mathrm{d}v}{\int_{V_{\mathrm{nonROI}}} \left|\overline{J}_{\mathrm{LE}}\right| \mathrm{d}v}, \quad (4)$$

where α is angle between the current source vector and lead vector at each location within ROI and β is angle between the noise current source vector and lead vector at each location within nonROI.

In (Eq. 4) we have simplified the original SNR equation based on the following assumptions. Firstly, the conductivity σ is reduced from the equation because ROI and nonROI are within the brain volume having constant conductivity. Secondly, the sources in EEG can be described as equivalent dipoles. We assume that the sources within the ROI can be replaced by an equivalent dipole vector $\overline{J}_i$, which has constant direction and magnitude. We also assume that the measurement set up is optimally selected and thus the sources within ROI are parallel to the sensitivities and thus the cos (α) equals one in each source location. Thirdly, spatially random dipoles have been applied to model the sources generating background EEG, i.e. noise [3, 10, 11]. Because the orientations or magnitudes of the random noise source dipoles cannot be estimated accurately, we approximate the magnitude of $\overline{J}_i$ within nonROI to be equal to one. In the worst case, the sources within nonROI are parallel to the sensitivities and thus the cos (β) equals one in each source location. Now, we observe that the estimation of SNR is proportional to the previously presented ROISR parameter in (Eq. 3). Next, we examine the relationship between the ROISRs and SNRs of two different leads.

Equation 5 presents the straight correlation between the ratio of ROISRs and ratio of SNRs of two different measurement leads, which are applied to the measurement of the same source.

$$\begin{aligned}\frac{\mathrm{ROISR}^1}{\mathrm{ROISR}^2} &= \frac{\frac{1}{V_{\mathrm{ROI}}}\int_{V_{\mathrm{ROI}}}|\overline{J}_{1,\mathrm{LE}}|\mathrm{d}v}{\frac{1}{V_{\mathrm{nonROI}}}\int_{V_{\mathrm{nonROI}}}|\overline{J}_{1,\mathrm{LE}}|\mathrm{d}v} \div \frac{\frac{1}{V_{\mathrm{ROI}}}\int_{V_{\mathrm{ROI}}}|\overline{J}_{2,\mathrm{LE}}|\mathrm{d}v}{\frac{1}{V_{\mathrm{nonROI}}}\int_{V_{\mathrm{nonROI}}}|\overline{J}_{2,\mathrm{LE}}|\mathrm{d}v} \\ &= \frac{\int_{V_{\mathrm{ROI}}}|\overline{J}_{1,\mathrm{LE}}|\mathrm{d}v}{\int_{V_{\mathrm{nonROI}}}|\overline{J}_{1,\mathrm{LE}}|\mathrm{d}v} \cdot \frac{\int_{V_{\mathrm{nonROI}}}|\overline{J}_{2,\mathrm{LE}}|\mathrm{d}v}{\int_{V_{\mathrm{ROI}}}|\overline{J}_{2,\mathrm{LE}}|\mathrm{d}v} \\ \frac{\mathrm{SNR}^1}{\mathrm{SNR}^2} &= \frac{|\overline{J}_{\mathrm{i}}|\cdot\int_{V_{\mathrm{ROI}}}|\overline{J}_{1,\mathrm{LE}}|\mathrm{d}v}{\int_{V_{\mathrm{nonROI}}}|\overline{J}_{1,\mathrm{LE}}|\mathrm{d}v} \div \frac{|\overline{J}_{\mathrm{i}}|\cdot\int_{V_{\mathrm{ROI}}}|\overline{J}_{2,\mathrm{LE}}|\mathrm{d}v}{\int_{V_{\mathrm{nonROI}}}|\overline{J}_{2,\mathrm{LE}}|\mathrm{d}v} \\ &= \frac{\int_{V_{\mathrm{ROI}}}|\overline{J}_{1,\mathrm{LE}}|\mathrm{d}v}{\int_{V_{\mathrm{nonROI}}}|\overline{J}_{1,\mathrm{LE}}|\mathrm{d}v} \cdot \frac{\int_{V_{\mathrm{nonROI}}}|\overline{J}_{2,\mathrm{LE}}|\mathrm{d}v}{\int_{V_{\mathrm{ROI}}}|\overline{J}_{2,\mathrm{LE}}|\mathrm{d}v} \end{aligned} \quad (5)$$

In (Eq. 5) ROISR^1 and SNR^1 corresponds to measurement lead one and ROISR^2 and SNR^2 to measurement lead two. The ROI volume is the same for both leads. Because of the two different leads, the lead vectors have different magnitudes, $\overline{J}_{1,\mathrm{LE}}$ and $\overline{J}_{2,\mathrm{LE}}$. In the latter equation, the $\overline{J}_i$ between the two different measurement setups is constant, because the source of the measurement is the same. Based on the assumptions, the correlation is assumed to be highest, very close to one, when ROI optimally covers signal sources and current source vectors are oriented parallel to the lead vectors within ROI or the directions of sources are applied in ROISR calculation.

2.5 Preliminary clinical study of the correlation between ROISR and SNR

We demonstrate here with a preliminary visual evoked potential (VEP) experiment, how well the ROISRs and the SNRs of real measurements correlate. The VEPs were measured with Neuroscan (SynAmp, Neuroscan) and 256-channel EEG cap containing 254 EEG channels and 2 ECG channels. The VEP experiment was based on checkerboard stimulation procedures described in [2]. The stimulations were made with Stim (Neuroscan). During the experiment, we measured 290 evoked responses (hereafter epochs). The measurements were conducted with two volunteers, male and female, hereafter testee 1 and testee 2, respectively.

The sensitivity distributions and further ROISRs for measurement leads of both testees were calculated with the three-layer spherical head model. The electrode locations applied in the calculations were digitized during the measurements with FastTrak (Polhemus) and fitted afterwards on the surface of the spherical model. Fig. 2 presents the numbering and locations of the centreline electrodes of testee 2.

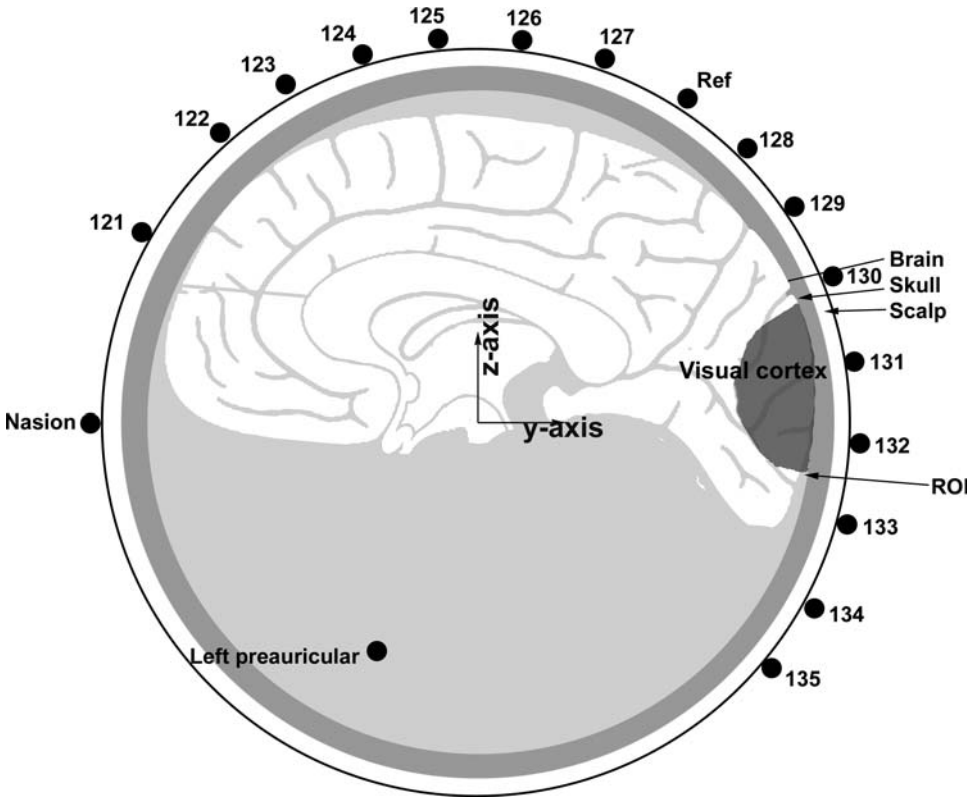

Fig. 2 Illustration of locations for electrodes 121 to 135 applied in the measurements and fitted on the spherical model. The region of interest is illustrated in *dark grey*

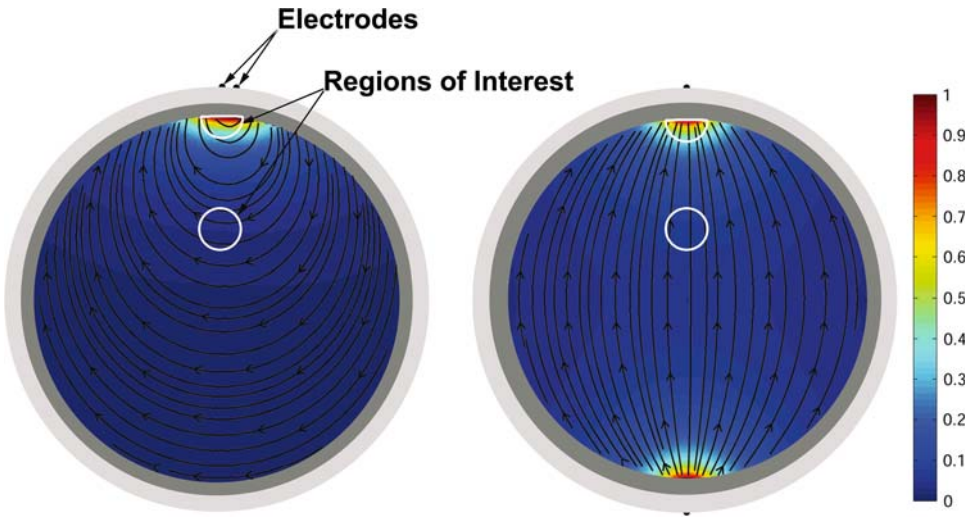

Fig. 3 Sensitivity distributions of the leads with 5.14° (*left*) and 180° (*right*) electrode distances in plane $y = 0$. Cortical ROI and deep ROI presented with *white*

SNRs of the measured VEPs were calculated with equations adopted from Raz et al. [20]. The interest was in the P100 component of VEP response and thus we calculated the SNRs of the time interval between 70 to 130 ms after the stimulus. For each lead 290 epochs were included in the calculation of SNRs.

The visual evoked responses are generated on the primary visual cortex which can be approximated to lie under electrodes 130–134 illustrated in Fig. 2 [23]. The highest correlations between ROISRs and SNRs could be achieved when the ROI is located in this region. We selected the ROI as a spherical segment of 20 mm radius on the cortex by observing anatomical images and previous studies of the size of primary visual cortex [1]. First we evaluated the correlation, by selecting the ROI volume to be located at the centre of the visual cortex, under the electrode 131 illustrated in Fig. 2. The ROISRs and SNRs were calculated for all 254 leads and applied in Eq. 6 to calculate the correlation coefficient between these quantities.

$$\text{correlation} = \frac{n\sum_n (XY) - \sum_n X \sum_n Y}{\sqrt{\left[n\sum_n X^2 - \left(\sum_n X\right)^2\right]\left[n\sum_n Y^2 - \left(\sum_n Y\right)^2\right]}} \quad (6)$$

where n is the number of data points (254 leads), X is the SNRs of 254 leads Y is the ROISRs of 254 leads.

We also studied how the location of ROI affects the correlation between ROISR and SNR and thus we calculated ROISRs for ROIs having centres on the centreline of the sphere under the electrodes from 121 to 135 illustrated in Fig. 2. We also studied how the correlation is affected when different source directions within ROI are assumed and applied in ROISR calculation. We applied the positive y- and z- directions as possible source directions within ROI.

3 Results

3.1 Effect of electrode distance

Figure 3 presents the normalized magnitudes and directions of sensitivities for electrode distances 5.14° (a) and 180° (b) on the yz-plane. Figure 4 presents the ROISRs calculated with (Eq. 2) for a cortical ROI (a) and a non-cortical ROI (b) as a function of the electrode distance. Figure 4 presents also the sensitivity ratios in cases where the sources are supposed to be in y- or z-direction within the ROI, these sensitivity ratios are called as ROISR_y and ROISR_z, respectively

From Fig. 3a it can be seen that with 5.14° electrode distance the sensitivity is high within the cortical region while on the other regions it is close to zero. In Fig. 3 it is also shown that the sensitivities within the cortical ROI are mostly oriented along the y-direction with 5.14° electrode distance and along the z-direction with 180° electrode distance. This is reflected in the values of the ROISR_y and ROISR_z presented in Figure 4a. It can be observed that when decreasing electrode distance, the measurement becomes more specific to the sources directed in either y-or z-direction, but with short enough electrode distances the specificity to the sources in z-direction begins to decrease.

Figure 1 shows the location of non-cortical ROI and Fig. 4b presents the ROISRs as a function of electrode distance for same ROI. The behaviours of the ROISR, ROISR_y and ROISR_z are seen to differ little bit from Fig. 4a. The ROISR_y starts to rise rapidly when electrode distance is decreased and the ROISR_z does not increase as the electrode distance is reduced, but instead it starts to decrease with electrode distances shorter than 100°.

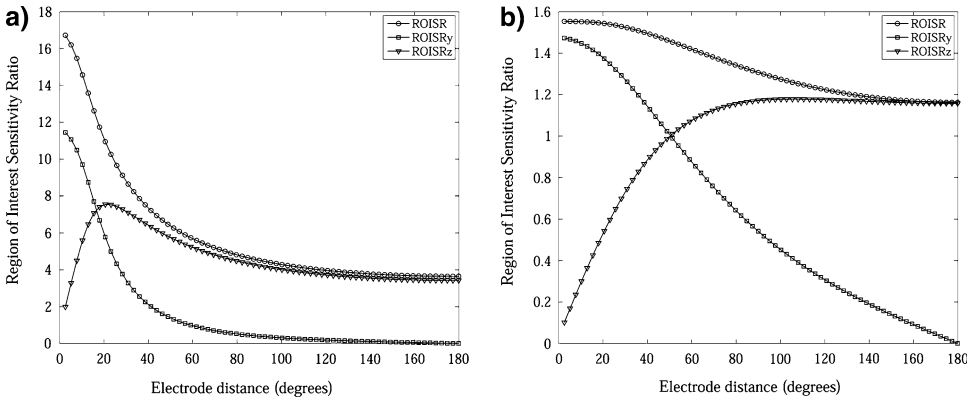

Fig. 4 ROISR, $ROISR_y$ and $ROISR_z$ as a function of interelectrode distance when the interest of measurement is on the sources within cortical ROI (**a**) and non-cortical ROI (**b**)

3.2 Correlation between ROISR and SNR

When the ROI was located under electrode 131, the correlations between ROISR and SNR for testees 1 and 2 were 82% and 94%, respectively. Figure 5 presents the correlations between ROISR and SNR as a function ROI location under electrodes 121–135 for both testees. The correlations were calculated with ROISRs applying three different assumptions of source orientations within ROI; unknown (a), positive *y*-axis (b) and positive *z*-axis (c). The ROISR and SNR have high correlations (> 75%) when the ROI is located under 131–134 but very low for other ROI locations. This observation corresponds to the assumptions made based on the knowledge of the location of primary visual cortex. Figure 5b shows that if the sources are assumed to be in positive *y*-direction high correlation between the $ROISR_y$ and SNR is achieved for the same ROI locations as in Fig. 5a. As presented in Fig. 5c, the correlations are notably lower when sources are assumed to be in positive *z*-direction.

4 Discussion

4.1 New ROISR parameter

In the present paper, we have introduced a concept of ROISR for analysing the ability of an EEG measurement setup to concentrate relatively high sensitivity on the predefined ROI. The results of this study are very promising, although we had limited number of testees and applied a three-layer spherical head model in sensitivity distribution calculations. Even though the spherical head models have been verified to be feasible in modelling EEG forward and inverse problems [16, 22], we will adopt realistically shaped head models in the future studies. In the future, we will also conduct studies with different evoked potentials and numbers of testees. More extensive study should also be conducted to find a way of selecting the correct ROI and how the size of the ROI affects the correlation between ROISR and SNR.

4.2 Effect of electrode distance

Electrode distance affects many properties of measurement sensitivity, and these effects are also dependent on the location of the ROI. The effects depend on whether the target source region is in the cortex or deeper in the brain. Malmivuo and Suihko [14] showed in their study that the spatial resolution of EEG is increased with shorter electrode distances and together with the present study we can state, that in general if the target region is on the cortex the electrode distance should be as short as possible. It should be noticed that Malmivuo and Suihko did not analyse the effect of the direction of sensitivity in their calculations. Based on the results presented here, we propose that the direction of the source should be considered in the measurement setup optimization, and the locations of the electrode should be adjusted above the ROI to obtain the optimal orientation. However, in many cases the electrodes can be arranged so that the sensitivity is optimally oriented.

4.3 Correlation between ROISR and SNR

The ideal situation to aim at in designing an electrode setup to measure bioelectric signals such as EEG, is to design a measurement configuration giving the highest possible SNR. Here, we demonstrated with a preliminary evoked potential study that the ROISR has a substantial correlation to the SNR of EEG leads when ROI is properly located. Similar correlation studies could be applied in the future to evaluate if the ROI is optimally selected, because correlation should be highest when the ROI contains all the signal sources and none of the noise sources. This approach could have some applications in source localization purposes.

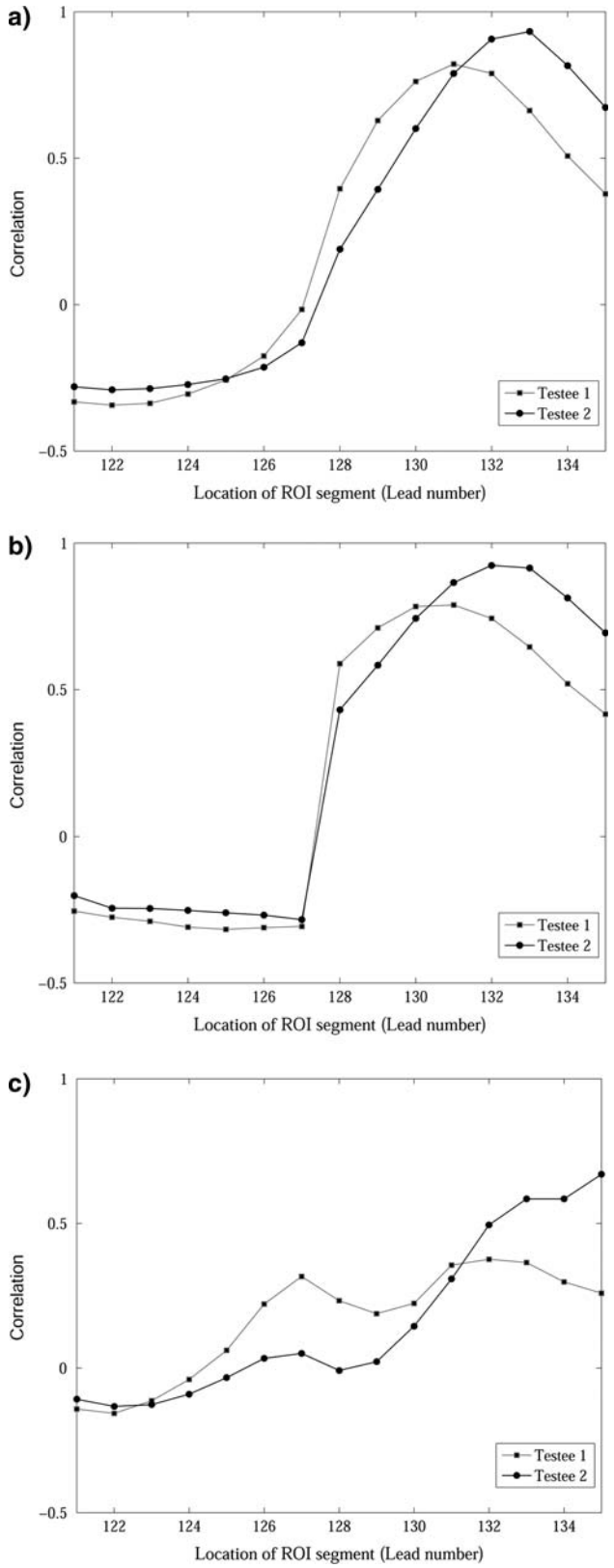

Fig. 5 Correlation between ROISR and SNR as a function of ROI location when orientation of sources is assumed to be unknown (**a**), positive *y* (**b**) and positive *z* (**c**)

Also, the direction of sensitivity has effect on the correlation and based on the theory behind ROISR, the highest correlation should be achieved when the proper direction of sensitivity is applied in the calculations and (Eq. 3) is used. The correlation studies between models and measurements could be applied to estimate the source directions within the ROI.

The results of this study imply that the sources producing P100 component in primary visual cortex are most likely oriented to the positive *y*-direction than to the positive *z*-direction because the correlation was higher when sensitivities to the positive *y*-direction were applied. Similar results of source directions have been achieved in previous studies where cortical dipole sources has been analysed and modelled [4–6, 8]. Even higher correlations might have been achieved with realistic models of testees' heads and with more precise assumptions of source orientation and ROI location.

5 Conclusions

In the present study we have introduced a new concept, ROISR, which describes how well the measurement is focused on the ROI and demonstrated the connection between ROISR and the SNR of measured EEG. We can conclude that ROISR serves an efficient modelling-based approach to evaluate EEG measurement setups. Although the method was applied only in analysing EEG measurements, we believe that the method is applicable in other bioelectrical measurements because it is based on the sensitivity distribution approach, which is universal for all bioelectrical sources.

Acknowledgements We would like to thank Robert MacGilleon for English proofreading. The work has been supported by grants from the Pirkanmaa Regional Fund of the Finnish Cultural Foundation, the Emil Aaltonen Foundation, the Foundation of Technology Finland and the Ragnar Granit Foundation.

References

1. Andrews TJ, Halpern SD, Purves D (1997) Correlated size variations in human visual cortex, lateral geniculate nucleus, and optic tract. J Neurosci 17(8):2859–2868
2. Celesia GG, Bodis-Wollner I, Chatrian GE, et al (1993) Recommended standards for electroretinograms and visual evoked potentials. Report of an IFCN committee. Electroencephalogr Clin Neurophysiol 87(6):421–436
3. de Munck JC, Vijn PC, Lopes da Silva FH (1992) A random dipole model for spontaneous brain activity. IEEE Trans Biomed Eng 39(8):791–804
4. Di Russo F, Martinez A, Sereno MI, et al (2002) Cortical sources of the early components of the visual evoked potential. Hum Brain Mapp 15(2):95–111

5. Di Russo F, Pitzalis S, Aprile T, et al (2006) Spatiotemporal analysis of the cortical sources of the steady-state visual evoked potential. Hum Brain Mapp
6. He B, Yao D, Lian J (2002) High-resolution EEG: on the cortical equivalent dipole layer imaging. Clin Neurophysiol 113(2):227–235
7. Hoekema R, Wieneke GH, Leijten FS, et al (2003) Measurement of the conductivity of skull, temporarily removed during epilepsy surgery. Brain Topogr 16(1):29–38
8. Ikeda H, Nishijo H, Miyamoto K, et al (1998) Generators of visual evoked potentials investigated by dipole tracing in the human occipital cortex. Neuroscience 84(3):723–739
9. Lai Y, van Drongelen W, Ding L, et al (2005) Estimation of in vivo human brain-to-skull conductivity ratio from simultaneous extra- and intra-cranial electrical potential recordings. Clin Neurophysiol 116(2):456–465
10. Lutkenhoner B (1998) Dipole source localization by means of maximum likelihood estimation I: theory and simulations. Electroencephalogr Clin Neurophysiol 106(4):314–321
11. Lutkenhoner B (1998) Dipole source localization by means of maximum likelihood estimation: II. experimental evaluation. Electroencephalogr Clin Neurophysiol 106(4):322–329
12. Malmivuo J, Plonsey R (1995) Bioelectromagnetism: principles and applications of bioelectric and biomagnetic fields. Oxford University Press, New York
13. Malmivuo J, Suihko V, Eskola H (1997) Sensitivity distributions of EEG and MEG measurements. IEEE Trans Biomed Eng 44(3):196–208
14. Malmivuo JA, Suihko VE (2004) Effect of skull resistivity on the spatial resolutions of EEG and MEG. IEEE Trans Biomed Eng 51(7):1276–1280
15. McFee R, Johnston FD (1953) Electrocardiographic leads I: introduction. Circulation 8(4):554–568
16. Neilson LA, Kovalyov M, Koles ZJ (2005) A computationally efficient method for accurately solving the EEG forward problem in a finely discretized head model. Clinical Neurophysiology 116(10):2302–2314
17. Niedermeyer E, Lopes da Silva F (1993) Electroencephalography: basic principles, clinical applications, and related fields. Williams and Wilkins, Baltimore
18. Nunez P (1981) Electric fields of the brain: the neurophysics of EEG. Oxford University Press, New York
19. Oostendorp TF, Delbeke J, Stegeman DF (2000) The conductivity of the human skull: results of in vivo and in vitro measurements. IEEE Trans Biomed Eng 47(11):1487–1492
20. Raz J, Turetsky B, Fein G (1988) Confidence intervals for the signal-to-noise ratio when a signal embedded in noise is observed over repeated trials. IEEE Trans Biomed Eng 35(8):646–649
21. Rush S, Driscoll DA (1969) EEG electrode sensitivity—an application of reciprocity. IEEE Trans Biomed Eng 16(1): 15–22
22. Vanrumste B, Van Hoey G, Van de Walle R, et al (2001) The validation of the finite difference method and reciprocity for solving the inverse problem in EEG dipole source analysis. Brain Topogr 14(2):83–92
23. Watson JDG (2000) The human visual system. In: Toga AW, Mazziotta JC (eds) Brain mapping: the systems. Academic Press, San Diego, pp 263–289
24. Väisänen J, Hyttinen J, Malmivuo J (2006) Finite difference and lead field methods in designing implantable ECG monitor. Med Biol Eng Comput 44(10):857–864